Modifying Wire-Array *Z*-Pinch Ablation Structure Using Coiled Arrays

G. N. Hall, J. P. Chittenden, S. N. Bland, S. V. Lebedev, S. C. Bott,* C. Jennings, J. B. A. Palmer, and F. Suzuki-Vidal

Blackett Laboratory, Imperial College, London SW7 2BW, United Kingdom

(Received 13 September 2006; revised manuscript received 9 October 2007; published 14 February 2008)

A new wire-array configuration has been used to control the modulation of ablated plasma flow for the first time. Cylindrical aluminum coiled arrays, in which each straight wire is replaced with a single helix, were driven by a 1 MA, 240 ns current pulse. Ablated plasma is directed away from the coiled wire cores in a manner that can be understood in terms of Lorentz forces that arise from a complex current path modeled by 3D magnetohydrodynamic simulations. Outside the diameter of the helix, the flow of ablated plasma is axially modulated at the wavelength of the coil.

DOI: 10.1103/PhysRevLett.100.065003 PACS numbers: 52.59.Qy, 52.38.Ph

The inertial confinement fusion community has shown great interest in the wire-array *Z* pinch as a radiation source for energizing hohlraums [1,2] since it provides an extremely powerful, energetic, and efficient source of x-rays (280 TW, 1.8 MJ achieved by the 20 MA *Z* generator at Sandia National Laboratories) [3]. Experiments have shown that the issue of the ablation of wires and the redistribution of mass prior to implosion is of fundamental importance to x-ray emission on all wire-array *Z* pinch machines with current from 1 MA to 20 MA [4–7].

The dominant feature of the ablation process is a quasiperiodic variation of the ablation rate along the wires, observed as plasma flowing from the wires in streams axially separated by a fundamental wavelength ($\lambda_f \approx 500\ \mu$m for Al, $\approx 250\ \mu$m for *W*) which varies with material [5]. The nonuniform breakup of wires that seeds instabilities which grow during implosion is a direct consequence of the nonuniformity of ablation rate. In cylindrical wire arrays this is ultimately responsible for the temporal spread of the start of implosion, and for the redistribution of mass during implosion, resulting in trailing mass and hence trailing current. Such modulations appear in all wire-array configurations in which ablated material experiences Lorentz ($\mathbf{J} \times \mathbf{B}$) forces arising from a global magnetic field. The quasiperiodic structure seen in array configurations is different from that observed in experiments with single wires [8] but is identical for all wire-array machines, with $\mathbf{J} \times \mathbf{B}$ forces varying by a factor of $\sim$400 [5–7], and is important for future machines.

Previous attempts to control ablation structure used chemical etching to produce a periodic modulation of the wire diameter with the aim of seeding perturbations at a wavelength different from the fundamental. This resulted in enhanced ablation at discontinuities in the wire diameter, but ablation flow modulated at the fundamental wavelength remained and was superimposed upon any additional flow structures at the etched wavelength [9].

In this Letter, we present the first observations of a method to change the fundamental ablation wavelength using a new array configuration in which all or some of the wires in a standard cylindrical array were replaced with wires prepared in a single-helix (coiled) geometry. This produces a significant change in the plasma flow structure from the wires; the fundamental wavelength was suppressed and replaced by ablation flow at the coil wavelength. Analysis suggests that the origin of the fundamental wavelength is a magnetohydrodynamic (MHD) instability.

Experiments were carried out on the MAGPIE generator [10], which produces a current pulse through the load that is closely approximated by $I(t) = I_0 \sin^2(\pi t/2\tau)$, where the peak current, I_0, of 1 MA is reached at $\tau = 240$ ns. The experimental setup is shown in Fig. 1(a). The nomenclature used to describe points on a coiled wire is explained in Fig. 1(b). The distance of each straight wire from the array axis was 8.5 mm, as was the distance from the axis of each coiled wire to the array axis. Coiled wire geometry is described by the pitch angle to the horizontal, ϕ, and the coil wavelength, λ_c. The diameter of a coil is $d = \lambda_c/\pi \tan\phi$. For these experiments, λ_c was varied between

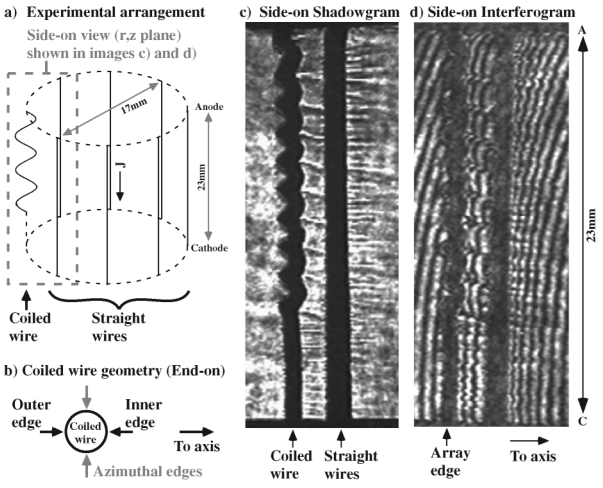

FIG. 1. (a) Experimental arrangement, shown for an array with 7 straight wires and 1 coiled wire. (b) Nomenclature used to describe points on a coiled wire. (c) Shadowgram and (d) interferogram at $t = 125$ ns. All wires are 25 μm Al, $\lambda_c = 1.7$ mm.

1.4 and 3.7 mm, while ϕ was maintained at ~45°. Laser probing (Nd-YAG, 532 nm, 0.4 ns) provided shadowgraphy and interferometry. Implosion trajectories were imaged using optical streak photography, and extreme ultraviolet (XUV) framing cameras (2 ns gate time, images radiation $\gtrsim$36 eV) provided time-resolved soft x-ray images. Photoconducting detectors filtered with 2 μm and 6 μm polycarbonate, 12.5 μm PVDC, 20 μm Be, and 6 μm Al measured x-ray intensity in five spectral bands.

The change in ablation structure that results from the use of coiled wires can be observed in laser probing images such as Fig. 1. These show a section of an 8-wire array containing a single coiled wire ($\lambda_c = 1.7$ mm) and 7 straight wires. In both these images, the straight wires, and the straight section of the coiled wire (near the cathode) exhibit ablation streams at the fundamental wavelength, which is ≈0.5 mm for aluminum. For the coiled section of the wire, however, the modulation of ablation at the fundamental wavelength is suppressed, and is replaced by ablation flow concentrated in narrow regions which occur periodically at the wavelength of the coil. Modulation of ablation flow at λ_c has, thus far, been demonstrated for coiled wires with λ_c between 1.4 and 3.7 mm (between ~2.8 and ~7.5 times the fundamental wavelength).

From Fig. 1 it appears that ablation streams from the coils originate from axial positions where the coil is furthest from the array axis (the "outer edge"), although from this figure it is not possible to see if this is the case close to the wire cores. The width of the streamers in the r, z plane is not particularly sensitive to λ_c and increases by only 0.3 mm (from ~0.7 to ~1 mm) when λ_c is increased from 1.7 to 3.7 mm. From interferometry, there appears to be very little plasma between the coil streamers; for the interferogram in Fig. 1(b) this density is sufficiently small as to produce less than 0.2 fringe shifts—the minimum sensitivity of the instrument ($n_e l < 8 \times 10^{16}$ cm^{-2}). However, each streamer from the coil produced ≈1 fringe shift which, using end-on probing to measure the path length (see Fig. 2), gives an estimate of the electron density between 1.3 and 3.3×10^{18} cm^{-3}. This is significantly higher than the density of streamers seen in straight arrays (typically of the order 10^{17} cm^{-3}).

Although laser probing indicates that the ablation streams are axially aligned with the outer edges, there is strong evidence that the outer edges are not the parts of the coil where ablation is most concentrated. The images in Fig. 2 show a section of the same 20 μm Al 8-wire array containing both coiled and straight wires. In Fig. 2(a) the strongest emission extends ~$\lambda_c/4$ above and below each of the inner edges, i.e., between those points on the coil which have maximum azimuthal displacement (the "azimuthal edges"). Strong emission observed in XUV images generally indicates the locations at which the majority of ablation is occurring [11]. This is confirmed by Figs. 2(b) and 2(c), which show wire breakage occurring at the azimuthal edges and that the initial movement of plasma

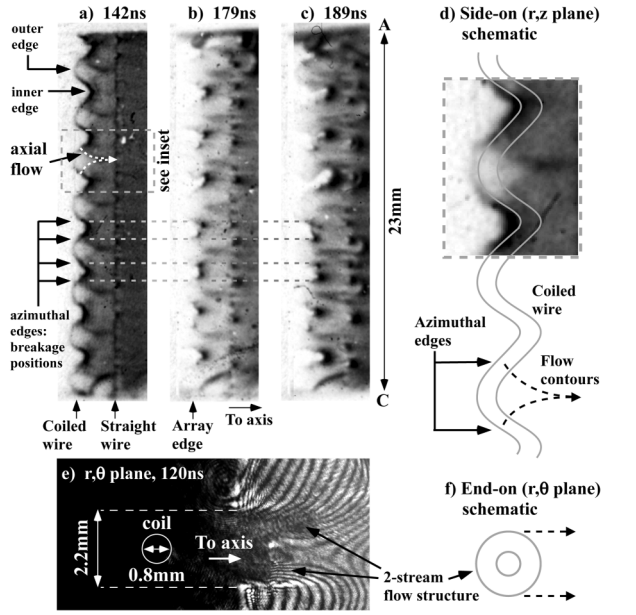

FIG. 2. XUV camera images of an imploding 20 μm coiled wire ($\lambda_c = 2.7$ mm). (a) Prior to implosion. (b) Wire breakage occurs at the azimuthal edges. (c) The outer edge remains as trailing mass. (e) End-on interferogram of the ablation flow. (d) Side-on and (f) end-on schematic of the observed flow structures.

as the implosion proceeds is aligned with these positions. Wire breakage at the azimuthal edges is consistent with an analysis of the $\mathbf{J} \times \mathbf{B}$ forces on a coiled wire, discussed in detail later. The outer edge remains in its initial position as trailing mass. It has previously been observed that for straight wires, axial positions of ablation streams are anticorrelated with axial positions at which wire core breaks develop [5,6], suggesting axial plasma motion. For coiled wires, Fig. 2 suggests axial plasma motion is also present, since the axial positions of ablation streams and wire breaks are different (although the mechanism is different and will be discussed in detail later). Figure 1 suggests that, once outside the vicinity of the wire cores, sufficient axial transport has occurred for the ablation streams to be aligned with the outer edges.

Figure 2(a) hints towards this complex redirection of mass, showing emission features that may indicate axial flow (labeled). These features suggest movement of plasma from the azimuthal edges upwards, downwards, and also towards the array axis, finally becoming aligned with the outer edges, as illustrated by the flow contours in Fig. 2(d). End-on laser probing [Fig. 2(e)] reveals that the r, θ profile of the ablation flow has a two-stream structure, illustrated in Fig. 2(f). From Fig. 2(e), the total width of this flow structure (in the r, θ plane) is ~2.2 mm for coils with $d =$ 0.8 mm ($\lambda_c = 2.7$ mm) constructed from 20 μm aluminum. End-on interferometry also shows that, in the r, θ plane, the width of this two-stream structure is large compared to the width of ablation streamers seen from straight wires of the same wire-diameter (~1.3 mm).

Calculations of the vacuum magnetic field produced by a coiled array reveal no topological features that explain this complex flow of plasma. Instead, the $\mathbf{J} \times \mathbf{B}$ forces responsible for these flow structures arise from complex current paths generated by the motion of ablated plasma.

Close to the wire cores, a helical current path results in a radial component of current, $\mathbf{J_r}$, which is directed either towards or away from the array axis as illustrated in Fig. 3(a). Combined with the global magnetic field ($\mathbf{B_g}$) this results in an axial force, $\mathbf{F_z} = [\mathbf{J_r} \times \mathbf{B_g}]_\mathbf{z}$, which is directed axially upwards on one side of the coil, and downwards on the opposite side, as illustrated in Fig. 3(a). Additionally, coronal plasma is directed radially away from the wire cores towards the array axis under the influence of the Lorentz force ubiquitous to wire arrays, $\mathbf{F_r} = [\mathbf{J_z} \times \mathbf{B_g}]_\mathbf{r}$. The global magnetic field varies approximately as $\mathbf{B_g} \approx \mu_0 I(n-1)/4\pi n R_c$, where n is the number of wires in the array and R_c is the radial distance of an element of the helix from the array axis. Therefore, since the diameter of the coils is small (hence R_c varies little), $\mathbf{F_r}$ is relatively uniform along the helix: for $\lambda_c =$ 1.4–3.7 mm, respectively, $\mathbf{F_r}$ is $\approx$ 1.05–1.15 times greater at the inner edges than at the outer edges. The combined effect of $\mathbf{F_z}$ and $\mathbf{F_r}$ is that the point on the coil at which the total $\mathbf{J} \times \mathbf{B}$ is maximum is approximately the same point at which $\mathbf{F_z}$ is maximum: the azimuthal edges. It is at these points on a coiled wire, the positions of maximum azimuthal displacement, that the wire core is most rapidly ablated and the plasma experiences the greatest force away from the helix. This initiates the flow suggested by the emission contours in Fig. 2(d) and results in wire breakage occurring at the azimuthal edges, as shown in Fig. 2(b). Figure 2(d) also shows that although plasma first moves away from the coils in a direction approximately perpendicular to the wire core, further downstream the flow has become almost horizontal, indicating that the direction of $\mathbf{F_z}$ has reversed. Simulations of coiled arrays using GORGON, a 3D radiative, resistive MHD code [12,13], suggest that the reversal of the $\mathbf{F_z}$ force is due to complex current paths through the ablated plasma. Figure 3(b) shows the simulated current paths near a section of coiled wire in an array, correctly predicting that at the azimuthal edges the $\mathbf{J} \times \mathbf{B}$ force is approximately perpendicular to the wire core and, in the axial direction, is directed away from axial positions aligned with the inner edges and towards axial positions aligned with the outer edges. As the plasma moves away from the wire core, the simulation shows that the axial direction of $\mathbf{J} \times \mathbf{B}$ undergoes a reversal, resulting in velocity streamlines which strongly resemble the emission contours in Fig. 2(a). The reversal of $\mathbf{F_z}$ is due to the current path through the ablated plasma acquiring a radial component opposite in direction to the helical current path close to the wire cores. As illustrated in Fig. 3(a), a stream of ablated plasma is directed downwards from one azimuthal edge by helical current flow, and a fraction of the current flows radially inwards along this stream, interacting with the global field to produce an upwards force. At the same time, a second streamer moves upwards from the opposite azimuthal edge, providing the radial return path for current which has moved inwards along the first streamer. Current moves from one streamer to the other through low density plasma in the region between them. The reversal of the $\mathbf{F_z}$ forces acts to make the streams horizontal, which occurs when they become axially aligned with the outer edge.

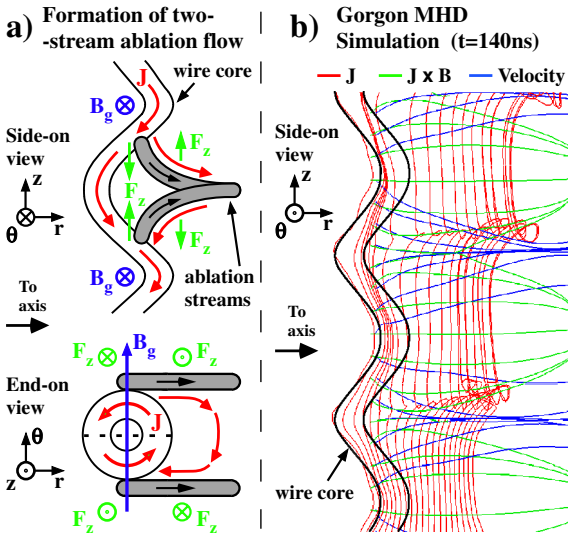

FIG. 3 (color online). (a) Schematic of the axial forces, $\mathbf{F_z}$, on current-carrying plasma close to a coiled wire core in an array, and also on the ablation streams. (b) GORGON 3D MHD simulation at $t = 140$ ns showing current, $\mathbf{J} \times \mathbf{B}$, and velocity streamlines in ablated plasma from a coiled wire ($\lambda_c =$ 3.7 mm) in an array.

It is possible to estimate, to some extent, the current division between helical paths close to the wire cores and other nonhelical paths through the ablated plasma such as those shown in Fig. 3(b). By assuming the axial magnetic field on the axis of a coiled wire ($\mathbf{B_z}$) is due solely to a helical current path close to the wire cores, the $\mathbf{B_z}$ predicted by GORGON at some time during the experiment can be compared to the field that would be produced by an ideal solenoid, $\mathbf{B_{is}}$. From the ratio $\mathbf{B_z}/\mathbf{B_{is}}$, the fraction of current following a helical path can then be estimated. Early after the start of the current ($t = 10$ ns) $\mathbf{B_z}/\mathbf{B_{is}} \approx 0.97$ as might be expected, and by $t = 30$ ns this has only decreased to $\approx$0.94, indicating that the current path at these times is almost completely helical. As the experiment proceeds further, this value begins to decrease rapidly: $\mathbf{B_z}/\mathbf{B_{is}} \approx 0.7$ at $t = 40$ ns. Later, the value of $\mathbf{B_z}/\mathbf{B_{is}}$ begins to vary significantly along the axis of the coils, becoming negative at axial positions aligned with the outer edges of the coiled wire. This is a result of the axial magnetic field produced by nonhelical current paths opposing the helical $\mathbf{B_z}$, and at this point it becomes difficult to accurately assess the division of current. Nevertheless, the observation that wire breakage occurs at the azimuthal

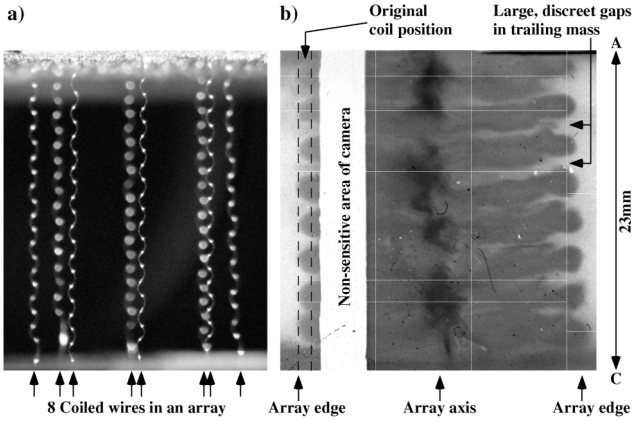

FIG. 4. (a) An 8-wire coiled array (20 μm Al, $\lambda_c \sim 2.7$ mm) prior to the start of current. (b) XUV camera image showing the implosion of this array at the time of x-ray peak (234 ns).

edges confirms that a substantial fraction of the current must remain in a helical path until the start of implosion.

Suppression of the fundamental wavelength and the generation of this new ablation structure was achieved by changing the topology of the magnetic field, strongly suggesting that the origin of the fundamental wavelength in straight arrays is related to the ability of MHD instabilities to form in the core-corona structure. Suppression of the fundamental wavelength in these experiments may be a result of the axial magnetic field generated by coiled wires (on the axis of a coil, $\mathbf{B_z}/\mathbf{B_g} \approx 4$–$11$ for $\lambda_c = 3.7$–1.4 mm, respectively), since the ability of such a field to stabilize Z pinch plasmas against the growth of $m = 0$ (sausage) and $m = 1$ (kink) MHD instabilities is well-known. The growth of such instabilities may also be reduced by shearing of the magnetic field around coiled wires. Magnetic shear (a change in the pitch angle of the total field) occurs both along the path of a coiled wire as the angle between the local and global fields changes and also tangentially to each element of a coiled wire as the relative strength of the local and global fields change.

In addition to addressing the issue of the origin of the fundamental wavelength, coiled arrays provide a method of imposing a predetermined, correlated perturbation as the initial conditions for the implosion phase. Axial correlation of the ablation streamers between individual wires is achieved simply by aligning all coils in an array such that the outer edges are at the same axial position. Additionally, large wavelength coils result in wire breaks with sufficient axial separation such that these perturbations do not merge axially during the implosion. This prevents the growth of the global instability from uncorrelated small scale perturbations that occurs during implosion of straight arrays. This effect is shown in Fig. 4, in which a coiled array (each wire aligned in the manner described above) is seen to implode, exhibiting the same wavelength of perturbation $\sim\lambda_c$ from the array edge to the array axis. The trajectory of the imploding material lies between that of the ablation streams, and therefore the implosion proceeds through relatively low density plasma, resulting in a continually accelerating implosion front with a maximum velocity $\sim$1.5 times that of a straight array with the same wire and array diameter. The effects of trailing current are likely to be mitigated by the large, correlated, discreet gaps which develop in the trailing mass, visible in Fig. 4(b). The result of the increased implosion velocity and the possibility of reduced trailing current is that, for large wavelength 8-wire coiled arrays, a dramatic increase in x-ray power is measured, equaling that of a 32-wire straight array on the MAGPIE generator. With these promising results, it is important to investigate how the performance of coiled arrays might scale to larger current and larger wire number arrays.

In conclusion, coiled arrays have been used to suppress the modulation of ablated plasma flow at the fundamental wavelength. Ablation flow in coiled arrays was seen to be modulated at the wavelength of the coil. Ablation flow from the coils is most rapid where the $\mathbf{J} \times \mathbf{B}$ forces on the coil are largest, which occurs at positions of maximum azimuthal displacement, resulting in a 2-stream flow structure in the r, θ plane and the implosion being initiated from these points. However, interaction of the global magnetic field with complex current paths in the ablated plasma results in axial transport which brings the ablation flow into axial alignment with the outer edges of the coil by the time the plasma has left the vicinity of the helix. These experiments suggest that the magnetic field topology is a key element responsible for the modulation of ablation of wires in a standard wire-array Z pinch, which may emerge as a result of MHD instabilities.

This research was sponsored by Sandia National Laboratories Albuquerque and the SSAA program of NNSA under DOE Cooperative Agreement No. DE-FC03-02NA00057.

*Present Address: University of California, San Diego, CA, USA.

[1] J. H. Hammer *et al.*, Phys. Plasmas **6**, 2129 (1999).
[2] M. K. Matzen *et al.*, Phys. Plasmas **12**, 055503 (2005).
[3] C. Deeney *et al.*, Phys. Rev. Lett. **81**, 4883 (1998).
[4] M. V. Bekhtev *et al.*, Sov. Phys. JETP **68**, 955 (1989).
[5] S. V. Lebedev *et al.*, Phys. Plasmas **8**, 3734 (2001).
[6] D. B. Sinars *et al.*, Phys. Plasmas **12**, 056303 (2005).
[7] M. E. Cuneo *et al.*, Phys. Rev. E **71**, 046406 (2005).
[8] D. H. Kalantar *et al.*, Phys. Rev. Lett. **71**, 3806 (1993).
[9] B. Jones *et al.*, Phys. Rev. Lett. **95**, 225001 (2005).
[10] I. H. Mitchell *et al.*, Rev. Sci. Instrum. **67**, 1533 (1996).
[11] S. V. Lebedev *et al.*, Plasma Phys. Controlled Fusion **47**, A91 (2005).
[12] A. Ciardi *et al.*, Phys. Plasmas **14**, 056501 (2007).
[13] J. P. Chittenden *et al.*, Plasma Phys. Controlled Fusion **46**, B457 (2004).